INVESTIGATION OF INHOMOGENEITY PARAMETERS OF ERS-2 WAVE MODE IMAGE

G. Song[(1),(2)], S. Lehner[(2)], J. Schulz-Stellenfleth[(2)],H. Grassl[(1)]
[(1)]*Univeristy of Hamburg Bundesstrasse 53, 20146 Hamburg, Germany, guiting.song@dlr.de*
[(2)]*German Aerospace Center (DLR), 82234 Wessling, Germany*

ABSTRACT

In order to classify different types of globally distributed synthetic aperture radar (SAR) wave mode images, which are acquired over the ocean for wind speed and sea state measurements, we develop a new scheme to differentiate images showing ocean wave, sea ice and surface slicks. A new classification parameter has been developed using 1535 SAR wave mode images to differentiate homogeneous and inhomoge-neous images. The new parameter is applied to two years of images. Comparison of the performance using the new parameter and inhomogeneity parameter (IH) defined in [1] are given. In the Arctic area the results of two parameters are compared to Special Sensor Microwave Imager (SSM/I) ice concentration data. The global distribution of inhomogeneous images is analyzed. Inhomegeneity in ice-free SAR images was found to be mainly due to low wind speed.

1 INTRODUCTION

It is has been demonstrated that synthetic aperture radar (SAR) images can be used to derive ocean wave parameters: significant wave height, mean wave period and wind speed [2]. An empirical approach (CWAVE) was developed at the German Aerospace Centre (DLR) to retrieve integral ocean wave parameters from SAR [2], the SAR image is the only input into the CWAVE algorithm. The homogeneity feature of the image is important for the results of CWAVE sea state measurements. Many studies have analyzed features of SAR images [3]-[4]. Several factors such as ice, atmospheric features like rain or biogenic surface films, oil slicks, or ship wakes can cause inhomogeneity. Such inhomogeneous images can not be used to retrieve wave parameters. Thus a homogeneity test has been developed in [1] based on standard spectral estimation theory. Every image has been divided into 32 sub-images of about 1 km×1 km size, which were then used to estimate the mean and variance of the periodograms. The expectation value of the homogeneity parameter θ (IH) is defined as follow:

$$\theta = \frac{\sum_k \overline{\mathrm{var}}(P_k)}{\sum_k \overline{mean}(P_k)} \Big/ \frac{\sum_k \overline{\mathrm{var}}(P_k)}{\sum_k \overline{mean}(P_k)} \qquad (1)$$

Where $\overline{mean}$ and $\overline{\mathrm{var}}$ are standard estimators for the periodograms mean and variances. P_k is the sub-image's periodogram. For a perfectly homogeneous image, the parameter θ should be 1, images were called inhomogeneous when IH>1.05. In most of cases, by using IH one can divide the images into classes of homogenous and inhomogeneous ones, but some cases have been detected, that are incorrectly classified even in the open ocean area. So a new classification scheme is needed. We further investigated the reason for the inhomo-geneity distribution over the global ocean, one obvious reason is occurrence of sea ice.

2 DATABASE

2.1 Wave mode ERS-2 image

The images used in this paper is wave mode ERS-2 images which are of 10 by 5 km size acquired every 200 km along the satellite track. The C-band radar operates with vertical polarization in transmit and receive and provides a spatial resolution of about 10 m in azimuth and 20 m in range. The required SAR wave mode single look complex (SLC) images, which are not available as standard products were reprocessed at DLR [4] from raw data provided by the European Space Agency (ESA). 1535 test images classified by visual inspection into four types: water, slick, ice and undefined images were used to develop new classification parameters as can be seen on Fig. 1. The newly-developed parameters are validated by nearly 1 million ERS-2 wave mode images from Sep. 1998 to Nov. 2000.

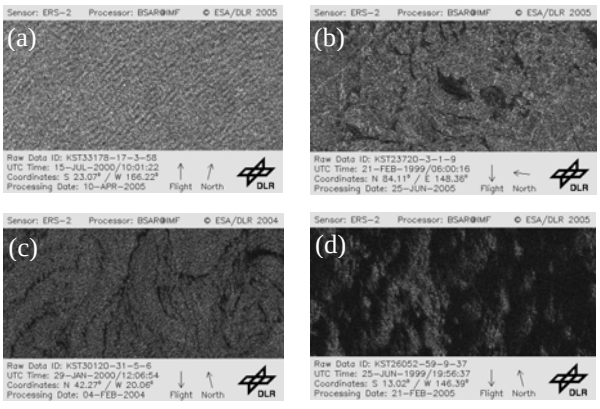

Figure 1. Four types of imagettes: (a) water (b) ice (c) slick (d) undefined

Proc. of "SeaSAR 2008", Frascati, Italy, 21-25 January 2008
(ESA SP-656, April 2008)

2.2 HOAPS wind speed and precipitation data

Wind speed and precipitation data of HOAPS atlas [5] are used in this paper. The spatial resolution is 0.25º×0.25º longitude/latitude and the temporal step is twice daily (0 UTC (0-12 UTC overpasses) and 12 UTC (12-24 UTC overpasses)). Each grid-cell contains the average of data from the satellite that passed this gridbox closest to 12 and 24 UTC, respectively. The time range of HOAPS data used here is from Sep. 1998 to Nov. 2000. Fig. 2 shows the mean wind speed from Sep. 1998 to Nov. 2000. It can be seen, that high average wind speed (U_{10}) occurs on several areas: circumpolar, North Atlantic and North Pacific.

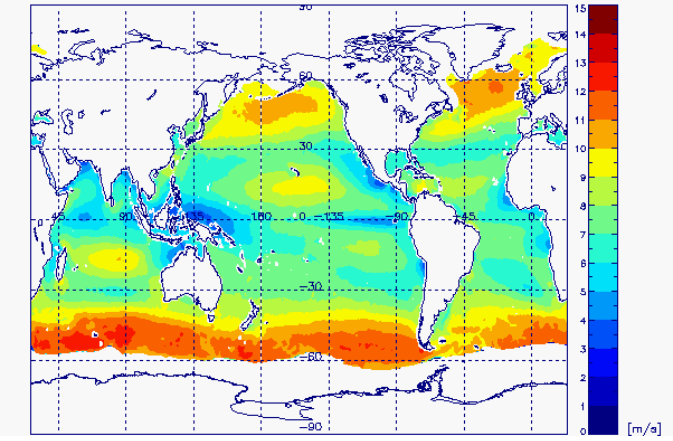

Figure 2. The mean wind speed between Sep. 1998 and Nov. 2000 from HOAPS with a spatial resolution 0.25º×0.25º longitude/altitude

2.3 SSM/I ice concentration data

The Special Sensor Microwave Imager (SSM/I) derived ice concentrations include Defense Meteorological Satellite Program (DMSP) F8, F11, and F13 daily and monthly sea ice concentrations, using the NASA Team algorithm, at a resolution of 25 km×25 km. The data used in this paper are collocated with SAR wave mode images [6].

3 NEW CLASSIFICATION PARAMETER DEVELOPING

3.1 The scheme of division of image

In a first classification scheme we consider the distribution of the intensity of sub-images in comparison to the mean intensity of the complete image. We choose the following division into sub-images, which gave us the best results. Every wave mode image contains 512 pixels in range direction with a resolution of 20 m and 1024 pixels in azimuth direction with a resolution of 4 m. In this scheme, 5 pixels are selected in range direction and 25 pixels are selected in azimuth direction in every sub-image, thus the size of sub-images is 100 m×100 m. There are 4080 sub-images in one wave mode image.

3.2 The definition of new parameters

Several new classification parameters are investigated in this paper. The definitions are as follows:

(1) **CoVar**: the variance of the intensity of every sub-image divided by the mean value of intensity of the whole image

(2) **Min**: The Minimum normalized radar cross section (NRCS) of sub-image. This is compared to the mean NRCS of the whole image.

(3) **Max**: The Maximum NRCS of sub-image. This is compared to the mean NRCS of the whole image.

(4) **PC (Percentile)**: Fig. 3 shows the sketch of the definition of PC. Eqs. 2-6 give the definition of PC. Mean, standard deviation and percentile are calculated from the intensity of every image pixel.

$$\bar{I} = < I > \quad (2)$$

$$\delta = std(I) \quad (3)$$

$$\eta = \bar{I} + 2\delta \quad (4)$$

$$n = where(I > \eta) \quad (5)$$

$$PC = \frac{n}{N} * 100\% \quad (6)$$

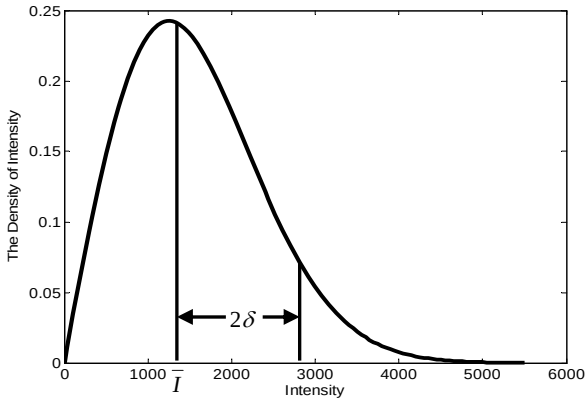

Figure 3. Sketch of the definition of Percentile (PC)

4 CLASSIFICATION PARAMETER SCHEME

The mean intensity of the whole image is plotted against Inhomogeneity parameter (IH (Fig. 4)), CoVar (Fig. 5), Min (Fig. 6), Max (Fig. 7), and PC (Fig. 8) for the 1535 test images. From visual inspection, data points marked by + are ocean water images, ones marked by * are ice images, ones marks by △ are

slick images, and ones marked by □ are undefined images. It can be seen that Min is the best parameter, for separation water images from other types of inhomogeneous images.

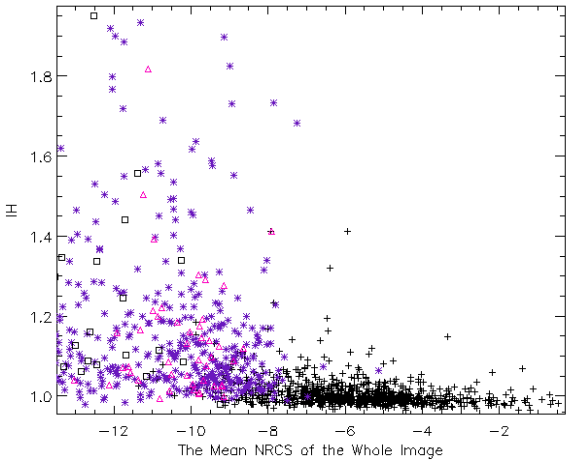

Figure 4. IH against the mean NRCS of the whole image, +: water *: ice △: slick □: undefined

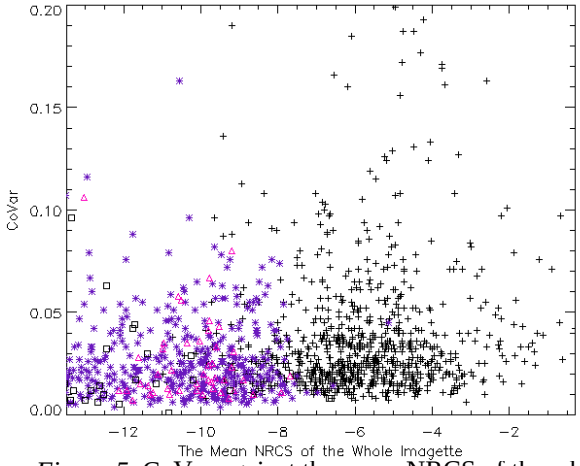

Figure 5. CoVar against the mean NRCS of the whole image, +: water *: ice △: slick □: undefined

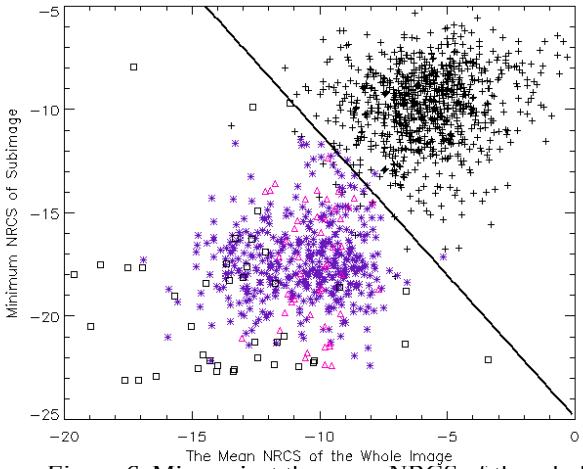

Figure 6. Min against the mean NRCS of the whole image, +: water *: ice △: slick □: undefined

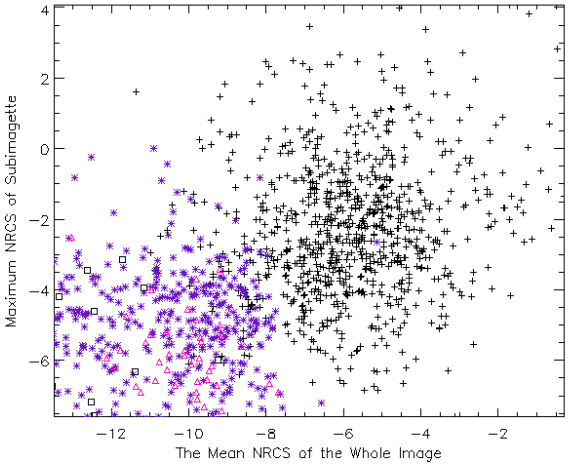

Figure 7. Max against the mean NRCS of the whole image, +: water *: ice △: slick □: undefined

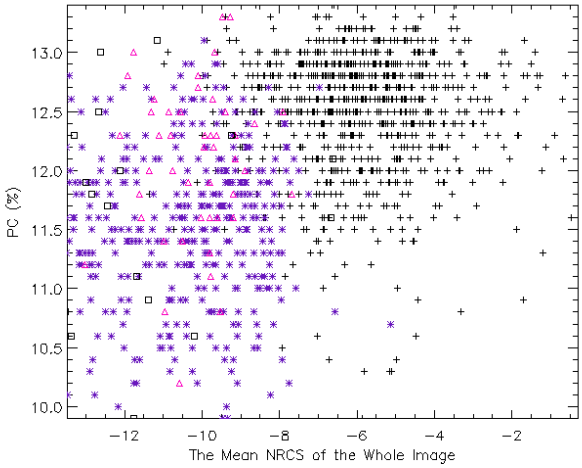

Figure 8. PC against the mean NRCS of the whole image, +: water *: ice △: slick □: undefined

After linear fitting, the separation function is:

$$y = -1.376x - 24.9 \quad (7)$$

where y is the minimum NRCS of the sub-images and x is the mean NRCS of the whole image. This separation function is applied to the two years images to separate the homogeneous images from inhomogeneous ones as a new classification parameter. The old parameter IH and CoVar do not add information to the separation by mean intensity. Max and PC show more misclassifications than Min when using a linear separation scheme. Best results are obtained using the Min parameter.

5 GLOBAL MAPS OF INHOMOGENEITY

The new classification scheme (Min) was applied to the two years ERS-2 images. All of the images are located in ocean areas. 3°×3° longitude/latitude boxes over the ocean are selected to investigate the global distribution of the inhomogeneous images. The percentage of inhomogeneous images in every box is calculated over the ocean. A global map of the percentage of inhomogeneity distribution between 0 and 40% is given in Fig. 9. The areas near the equator of the West Pacific Ocean (90°E-150°E, 20°S-20°N), the West America coastal (135°W-90°W, 0°-30°N), the South Indian Ocean (46°E-80°E, 3°S-10°N) and Northwest Africa coastal (20°W-10°W, 3°N-15°N) show a high number of inhomogeneous images.

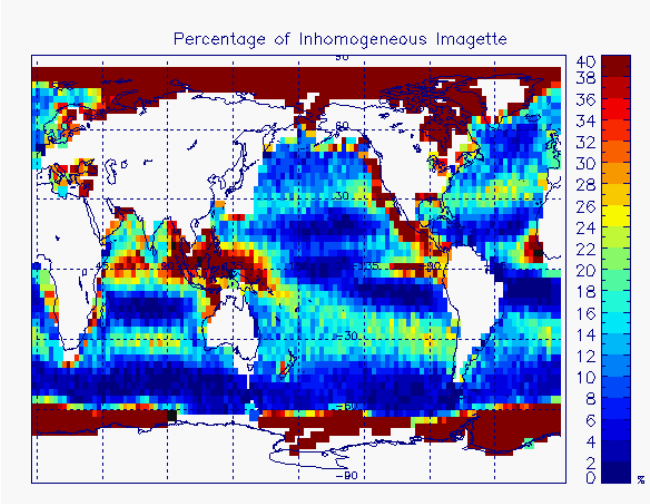

Figure 9. Global map of percentage of inhomogeneous images on 3°×3° boxes using the new classification parameter (Min) up to 40% or higher

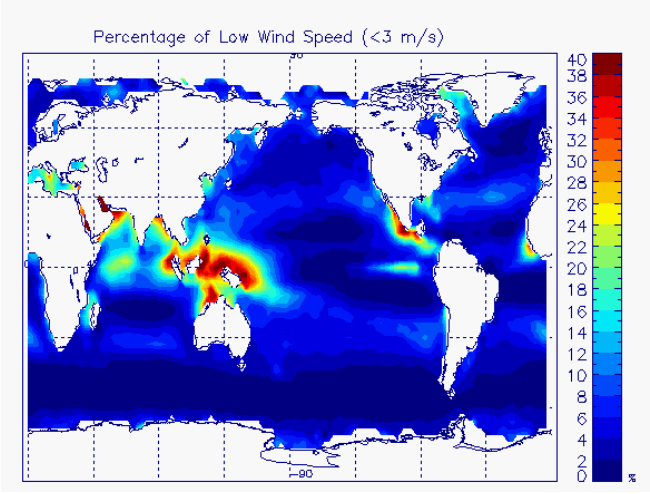

Figure 10. Global distribution of low wind speed (<3 m/s) on 3° ×3° longitude/latitude boxes from HOAPS

The main reason of such strong inhomogeneous distribution in the area is possibly low wind speed as shown in Fig. 10, which gives HOAPS low wind speed (below 3 m/s) distribution. The mean precipitation from Sep. 1998 to Nov. 2000 in Fig. 11 shows a different distribution, this will be investigated further for individual cases.

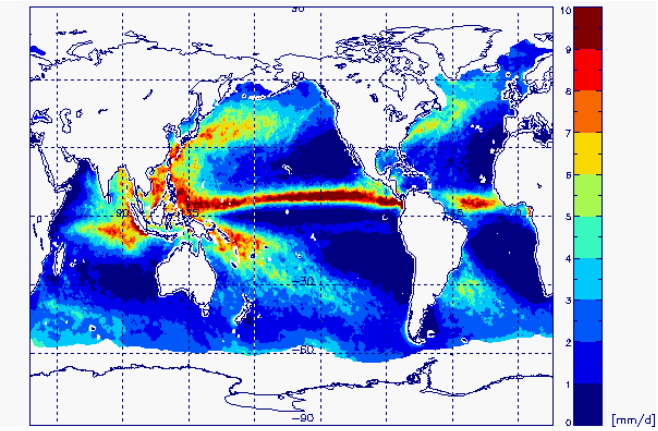

Figure 11. Global distribution of the mean precipitation from HOAPS between Sep. 1998 and Nov. 2000

6 SEA ICE

In order to discriminate the inhomogeneity in the sea ice region, we plot the percentage of inhomogeneous images for the range between 40% and 100%. The percentage of inhomogeneous images of the new classification parameter in the Arctic area is much higher than that of IH, this seems to indicate that the new classification parameter is more rigorous than IH.
To further investigate this, SSM/I ice concentration data of the Arctic area are compared. Fig. 12 shows a comparison of the percentage of inhomogeneous images in polar region of the new classification parameter (Min), IH and the mean SSMI concentration. It can be observed, that the results of the new classification parameter fits better to the SSM/I concentration data than that of IH in the Arctic area. The high mean SSMI concentration in the Arctic area corresponds to the high inhomogeneous images' distribution.
This will be further investigated to derive parameters on sea ice properties.

7 CONCLUSIONS

Different parameters to classify SAR images inhomogeneity are investigated in this paper to better distinguish inhomogeneous and homogeneous images for sea state measurements. A new separation function using mean of the image and minimum of a sub-images is given. The global distribution of inhomogeneous images of both the new classification parameter and IH are analyzed and compared to the global low wind

speed distribution as given by the HOAPS data. In the Arctic area the distribution of inhomogeneous images are compared to the SSM/I ice concentration data.

(a)

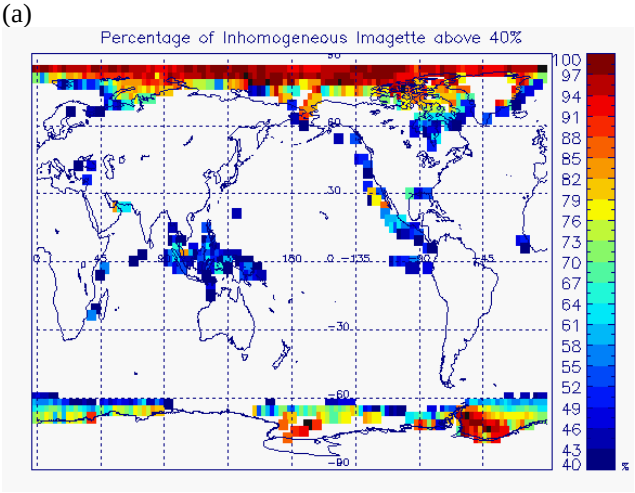

(b)

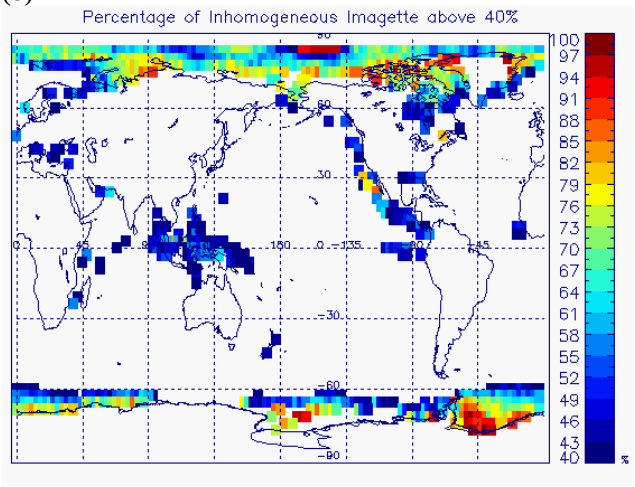

Figure 12. Global distribution of inhomogeneous images with 3° ×3° longitude/latitude boxes, (a) new classification parameter (b) IH parameter

(a)

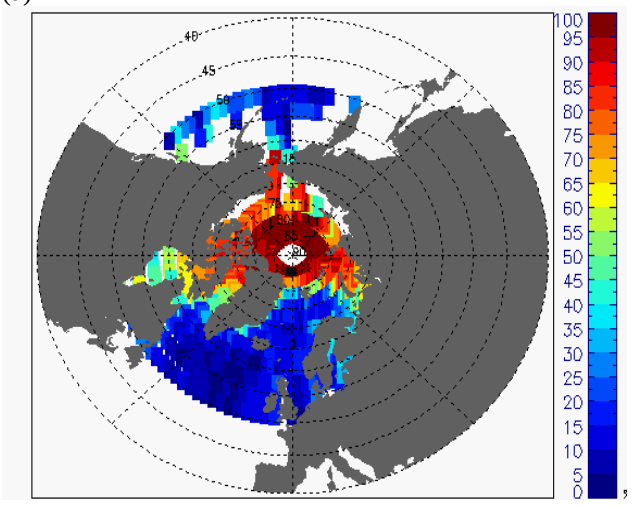

(b)

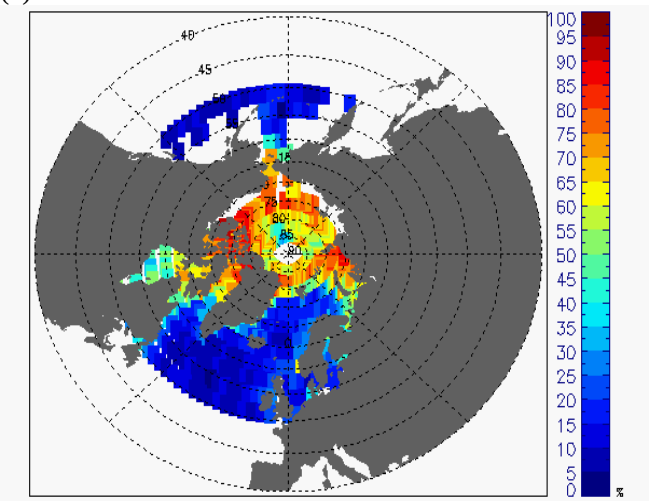

(c)

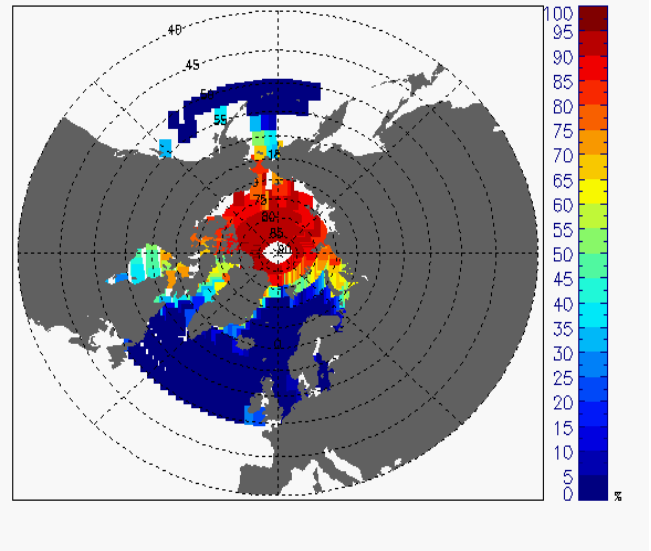

Figure 13. Percentage of inhomogeneous images in the Arctic region (a) by the new classification parameter (b) by the IH parameter (c) SSM/I ice concentration

This new scheme improves the flagging for SAR images used in the empirical algorithm CWAVE that determine sea state from SAR images. In the future we will analyze individual cases that are not due to low wind speed in relation to rain rate and sea surface temperature.

8 ACKNOWLEDGEMENTS

The analysed wave mode images were provided by ESA in the framework of the WAVEATLAS (ID 2342) PROJECT.

9 REFERENCES

1. Schulz-stellenfleth J. & Lehner S. (2004). Measurement of 2-d Sea Surface Elevation Fields Using Complex Synthetic Aperture Radar Data. *IEEE Trans. Geosci. Remote Sens.* **42**, 1149-1160.

2. Schulz-stellenfleth J., koenig T. & Lehner S. (2007). An Empirical Approach for the Retrieval of Integral Ocean Wave Parameters from Synthetic Aperture Radar Data. *J. Geophys. Res.* **112**, 3019-3033.

3. Horstmann J., Schiller H., Schulz-stellenfleth J. & Lehner S. (2003). Global Wind Speed Retrieval from SAR. *IEEE Trans. Geosci. Remote Sens.* **41**, 2277-2286

4. Lehner S., Schlut.stellenfleth J., Schaettler B., Breit H. & Horstmann J. (2000). Wind and Wave Measurements Using Complex ERS-2 SAR Wave Mode Data. *IEEE Trans. Geosci. Remote Sensing*. **38**(9), 2246–2257.

5. Grassl H., Jost V., Kumar R., Schulz J., Bauer P.& Schluessel P. (2000). The Hamburg Ocean-Atmosphere Parameteres and Fluxes from Satellite Data (HOAPS): A Climatological Atlas of Satellite-Derived Air-Sea-Interaction Parameters over the Oceans. Report No.312, ISSN: 0937-1060, Max Planck Institute for Meteorology, Hamburg

6. Markus T. & Cavalieri D. J. (2000). An Enhancement of the NASA Team Sea Ice Algorithm. *IEEE Trans. Geosci. Rem. Sens.* **38**(3), 1387-1398.